HHS Public Access

Author manuscript

J Allergy Clin Immunol. Author manuscript; available in PMC 2021 September 01.

Published in final edited form as:

J Allergy Clin Immunol. 2020 September ; 146(3): 571–582.e3. doi:10.1016/j.jaci.2020.03.039.

Early life heterologous rhinovirus infections induce an exaggerated asthma-like phenotype

Charu Rajput, PhD[#1], **Mingyuan Han, PhD**[#1], **Tomoko Ishikawa, MS**[1], **Jing Lei, BS**[1], **Seyedehzarifeh Jazaeri, MD**[1], **J. Kelley Bentley, PhD**[1], **Marc B Hershenson, MD**[#1,2]

[1]Department of Pediatrics, University of Michigan Medical School

[2]Department of Molecular and Integrative Physiology, University of Michigan Medical School

[#] These authors contributed equally to this work.

Abstract

Background: Early-life wheezing-associated respiratory tract infection by rhinovirus (RV) is a risk factor for asthma development. Infants are infected with many different RV strains per year.

Objective: We previously showed that RV infection of 6 day-old BALB/c mice induces a mucous metaplasia phenotype which is dependent on type 2 innate lymphoid cells (ILC2s). We hypothesized that early-life RV infection alters the response to subsequent heterologous infection, inducing an exaggerated asthma-like phenotype.

Methods: Wild type BALB/c mice and *Rora*$^{fl/fl}$*Il7r*^{cre} mice lacking ILC2s were treated as follows: 1) day 6 of life sham + day 13 of life sham; 2) day 6 RV-A1B + day 13 sham; 3) day 6 sham + day 13 RV-A2; and 4) day 6 RV-A1B + day 13 RV-A2.

Results: Mice infected with RV-A1B at 6 days and sham at 13 days showed increased BAL eosinophils and mRNA expression of IL-13 but not IFN-γ, indicative of a type 2 immune response, whereas mice infected with sham on day 6 and RV-A2 on day 13 of life demonstrated increased IFN-γ expression, a mature antiviral response. In contrast, mice infected RV-A1B on day 6 prior to RV-A2 infection on day 13 showed increased eosinophils, mRNA expression of IL-13, IL-5, Gob5, Muc5b and Muc5ac, expansion of IL-13-producing ILC2s and exaggerated mucus metaplasia and airways hyperresponsiveness. *Rora*$^{fl/fl}$*Il7r*^{cre} mice showed complete suppression of BAL eosinophils and mucous metaplasia compared to *Rora*$^{fl/fl}$ mice.

Conclusion: Early-life RV infection alters the response to subsequent heterologous infection, inducing intensified asthma-like phenotype which is dependent on ILC2s.

Capsule Summary:

Early-life wheezing with rhinovirus (RV) is associated with asthma, and infants are infected with many RV strains. RV infection of immature mice alters the immune response to subsequent heterologous infection, causing an exaggerated asthma-like phenotype.

Corresponding author: Marc B. Hershenson, Medical Sciences Research Building II, 1150 W. Medical Center Drive, Ann Arbor, MI; Phone, 734-936-4200; Fax, 734-764-3200; mhershen@umich.edu.

Declaration of Interests: The authors declare no competing interests

Keywords

Asthma; childhood; early-life; IL-13; rhinovirus; RV-A1B; RV-A2; trained immunity; type 2 innate lymphoid cell (ILC2)

Introduction

Early-life wheezing-associated respiratory tract infections by human rhinovirus (RV) and respiratory syncytial virus (RSV) are considered risk factors for asthma development [1-7]. Children are infected with many different RV strains, with infants having 6-10 distinct RV infections per year [8]. RV infections do not induce specific immunity to reinfection by heterologous serotypes, even if viruses are from the same species, for example RV-A1A and RV-A2 [9, 10]. RVs are divided into three species (A, B and C) which comprise over 160 antigenically distinct strains. Recurrent RV infections could result in greater degrees of airway inflammation and the potential for airway remodeling and loss of lung function over time [5, 11, 12].

In the Tucson Children's Respiratory Study, a prospective birth cohort study, lower respiratory tract illness with RSV before 3 years of age was an independent risk factor for the development of wheezing up to age 11 years but not 13 years [6]. Infants with severe RSV [7] and RV [1] infections requiring hospitalization are more likely to have asthma at ages 13 and 7 years, respectively. In the University of Wisconsin Childhood Origins of Asthma birth cohort of infants at increased risk of asthma, wheezing with RV in the first three years of life was strongly associated with asthma at 6 and 13 years of age. [2, 4, 13]. In contrast to RV, the impact of RSV lessened with time. RV and allergic sensitization had additive effects on asthma risk. In the Western Australian Pregnancy Cohort Study, wheezing lower respiratory illness in the first year of life increased the risk for asthma at 6 years of age in both non-atopic and atopic children [14]. In the Perth Childhood Asthma Study of children at high atopic risk, asthma at 5 years of age was associated with early-life wheezy and/or febrile lower respiratory tract infection [15]. However, associations were restricted to children who displayed allergen sensitization. In the Netherlands Generation R study, children those with bronchitis, bronchiolitis and pneumonia before 3 yrs of age were more likely to have asthma and lower lung function at 10 yrs of age [12]. Allergic sensitization did not factor into the associations seen. Together these data suggest that early life respiratory viral infection, in particular with RV, may contribute to the development of asthma, in some cases in the absence of allergen sensitization.

Infection of immature mice with RSV predisposes to the development of IL-13-dependent airway eosinophilia and airways hyperresponsiveness after homologous reinfection five weeks later, whereas infection at weaning protects against reinfection [16, 17]. These data are consistent with the notion that early-life RSV infection polarizes the adaptive immune response in such a way that homologous reinfection stimulates type 2 immune responses. However, the effect of early-life heterologous RV infections, which are much more common, has not been studied. We have previously shown that RV infection of six day-old BALB/c mice, but not mature mice, induces an asthma-like phenotype which is associated with type

2 innate lymphoid cells expansion and dependent on IL-13, IL-25 and IL-33 [18, 19]. We found that ILC2s persisted greater than three weeks after infection [18]. These data are consistent with the notion that, following early-life RV-induced expansion, ILC2s could form a stable population of innate immune cells capable of responding to subsequent heterologous infections, a form of trained immunity [20].

To examine the effects of heterologous RV infections on airway responses, we infected immature mice with different RV strains (RV-A1B and RV-A2) on days 6 and 13 of life, measuring airway responses one week after the second infection. We hypothesized that day 6 RV-A1B infection would alter the immune response to heterologous infection with RV-A2 on day 13 of life, inducing an exaggerated asthma-like phenotype. We found that early-life heterologous infection with RV-A1B and RV-A2 induced intensified type 2 eosinophilic inflammation and mucous metaplasia which was dependent, at least in part, on ILC2s.

Methods

Animals.

All animal usage was approved by the Institutional Animal Care and Use Committee and followed guidelines set forth in the Principles of Laboratory Animal Care from the National Society for Medical Research. BALB/c mice were purchased from Jackson Laboratory (Bar Harbor, ME) and bred in house in pathogen-free facility within the Unit for Laboratory Animal Medicine at the University of Michigan. The *Rora*$^{fl/fl}$, *Rora*$^{fl/fl}$*IL7R*^{cre} and *IL7R*^{cre} mice were a gift from Dr. Andrew Mckenzie (MRC Laboratory of Molecular Biology, Cambridge, UK). Six day-old mice were used for the experiments.

Generation of RV-A1B and RV-A2.

RV-A1B and RV-A2 (ATCC, Manassas, VA), minor group viruses that infect mouse cells [21], were partially purified from infected HeLa cell lysates by means of ultrafiltration with a 100-kDa cutoff filter and titered by using a plaque assay as described previously [22, 23]. Intact virus does not go through the filter and is concentrated. Similarly concentrated and purified HeLa cell lysates were used for sham infection.

RV infections.

Mice were inoculated with 20 μl of 1 x 10^8 plaque-forming units (pfu) or sham HeLa cell lysate through the intranasal route under Forane anesthesia. Mice were treated on day 6 of life with RV-A1B and day 13 of life with RV-A2 as follows: 1) day 6 sham + day 13 sham; 2) day 6 RV-A1B + day 13 sham; 3) day 6 sham + day 13 RV-A2; and 4) day 6 RV-A1B + day 13 RV-A2 (Figure 1A).

Real-time quantitative PCR.

Lungs were harvested at day 20 of life (seven days after the last treatment) and RNA was extracted with Trizol (Invitrogen, Carlsbad, CA). Lung RNA was isolated using an RNAeasy kit (Qiagen). cDNA was synthesized from 2 μg of RNA using high capacity cDNA synthases kit (Applied Biosystems, Foster City, CA) and subjected to quantitative real-time PCR using specific primers for mRNA. The level of gene expression for each sample was normalized to

GAPDH. Sex was determined by *SRY (sex-determining region Y*) gene expression. To quantify virus particles, qPCR for positive-strand viral RNA was conducted using RV-specific primers and probes (forward primer: 5'-GTGAAGAGCCSCRTGTGCT-3'; reverse primer: 5'-GCTSCAGGGTTAAGGTTAGCC-3'; probe: 5'-FAM-TGAGTCCTCCGGCCCCTGAATG-TAMRA-3').

Lung histology and immunofluorescence.

Lungs were harvested at day 20 of life, fixed with 10% formaldehyde overnight and paraffin embedded. Blocks were sectioned at 500 μm intervals at a thickness of 5 μm, and each section was deparaffinized, hydrated and stained. To visualize mucus, sections were stained with periodic acid-Schiff (PAS; Sigma-Aldrich, St. Louis, MO). Other lung sections were stained with 4′,6-diamidino-2-phenylindole (DAPI) and Alexa Fluor 488-conjugated mouse anti-Muc5ac (clone 45M1; Thermo Fisher Scientific, Waltham, MA) or Alexa-Fluor 488-conjugated anti-CCL11 (Biolegend, San Diego, CA). IL-13-producing ILC2s and T cells were identified in the airways by immunofluorescence. Lung sections were stained with DAPI, Alexa Fluor 488-conjugated mouse anti-GATA3 (Biolegend), Alexa Fluor 647-conjugated mouse anti-CD3 (Biolegend) and Alexa Fluor 750-conjugated mouse IL-13 (R&D, Minneapolis, MN). AlexaFluor N-hydroxy succinimidyl esters were purchased from Thermo Fisher. ILC2s were identified as IL-13- and GATA3-positive, and T cells were identified as IL-13-, GATA3- and CD3-positive.

Images were visualized using Axioplan ApoTome microscope with appropriate filters (Carl Zeiss, Thornwood, NY). Muc5ac staining in the airway epithelium, ILC2s and CD3+ T cells were quantified by NIH ImageJ software (Bethesda, MD). Four separate mouse lungs from each of the four conditions were processed for sectioning. One section from the mid-left lung was analyzed from each mouse. Three-to-five separate airways of similar size from each lung were chosen for analysis. Muc5ac expression was calculated as the fraction of Muc5ac-positive epithelium compared with the total basement membrane length. For cell counts, the average number of cells per airway for each lung is shown.

Bronchoalveolar lavage (BAL).

Differential counts of BAL inflammatory cells were performed as described previously [24].

Flow cytometric analysis.

Lungs were perfused with PBS containing EDTA and minced and digested in collagenase IV. Cells were filtered and washed with RBC lysis buffer. For staining with anti-IL-13 antibody, the cells were incubated for 3 h with cell stimulation cocktail and protein transport inhibitors. Nonspecific binding was blocked by 1% fetal bovine serum with 1% LPS-free bovine serum albumin in DMEM, and 5 μg rat anti-mouse CD16/32 (Biolegend) was added. To identify ILC2s, cells were stained with FITC-conjugated antibodies for lineage markers CD3ε, TCRβ, B220/CD45R, Ter-119, Gr-1/Ly-6G/Ly-6C, CD11b (Biolegend), CD11c (Biolegend), TCRβ (Biolegend), F4/80 (Biolegend), and FcεRIα (Biolegend), anti-CD25-peridinin-chlorophyll-protein complex (PerCP)-Cy5.5 (eBioscience), and anti-CD127-allophycocyanin (APC; eBioscience), as described [18]. After staining for cell surface antigens, dead cells were stained with DAPI for flow sorting with live cells or Pac-Blue

Live/Dead fixable dead staining dye for further staining with anti-IL-13 antibody (eBioscience). For IL-13 staining, cells were fixed and permeabilized using permeabilization buffer (eBioscience) and stained with phycoerythrin (PE)-labeled anti-IL-13 antibody (eBioscience). Cells were subjected to flow cytometry on a LSR Fortessa (BD Biosciences, San Jose, CA), or sorted on a FACSAria II (BD Biosciences, San Jose, CA). Sorted lung ILC2s were cultured *in vitro* and then stimulated with cell stimulation cocktail (PMA and ionomycin from eBioscience) or recombinant mouse IL-33 (50ng/mL; Biolegend). Data were collected using FACSDiva software (BD Biosciences, San Jose, CA) and analyzed using FlowJo software (Tree Star, Ashland, OR).

Measurement of airway responsiveness.

Mice were anesthetized, intubated, and ventilated with a Buxco FinePointe System (Wilmington, NC). Mice were administered increasing doses of nebulized methacholine to assess airways responsiveness, as previously described [22].

Data analysis.

All data were represented as mean ± standard error (SE). For studies of airway responsiveness, statistical significance was assessed by two-way analysis of variance. For all other experiments, statistical significance was assessed by one-way analysis of variance. Group differences were pinpointed by the Tukey multiple comparison test.

Results

Heterologous RV infection induces exaggerated airway responses.

We found that RV infection of six day-old BALB/c mice, but not mature mice, induces an asthma-like phenotype which is associated with type 2 innate lymphoid cells expansion and dependent on IL-13, IL-25 and IL-33 [18]. However, the effects of early-life heterologous infection are unknown. Mice were treated on day 6 of life with RV-A1B and day 13 of life with RV-A2 as follows (Figure 1A): 1) day 6 sham + day 13 sham; 2) day 6 RV-A1B + day 13 sham; 3) day 6 sham + day 13 RV-A2; and 4) day 6 RV-A1B + day 13 RV-A2. Mice were sacrificed and lungs harvested at day 20. As seen previously, early-life RV-A1B infection (at day 6 of age) increased total lung mRNA expression of the ILC2 products IL-5 and IL-13 and the mucus-related genes Muc5ac, Muc5b and Gob5 (Figure 1B). In contrast, later infection with RV-A2 (on day 13 of life) failed to increase mRNA expression of these genes. IFN-γ mRNA was induced after late RV-A2 infection but not early RV-A1B infection, consistent with a mature antiviral response [18]. When we did the reverse experiment and infected six day-old mice with RV-A2 and 13 day-old mice with RV-A1B, we got similar results (Supplemental Figure 1).

Next, mice underwent heterologous infection with RV-A1B on day 6 of life and RV-A2 on day 13 of life. These mice demonstrated exaggerated total lung IL-5, IL-13, Muc5ac, Muc5b and Gob5 mRNA expression which was significantly higher than that induced by RV-A1B alone (Figure 1B). These data suggest that early-life RV-A1B infection shifted the response to subsequent RV-A2 infection from a type 1 to type 2 response. Consistent with this, IFN-γ mRNA expression was not increased in mice infected with RV-A1B prior to day 13 RV-A2

infection. However, total lung mRNA expression of TNF and IL-12b was also exaggerated in mice infected with both RV-A1B and RV-A2. These data show that the effect of heterologous infection does not strictly fit a type 2 model.

Next, we examined BAL inflammatory cell counts in RV-A1B and RV-A2 treated mice. As shown previously, RV-A1B infection on day six of life significantly increased BAL eosinophils (Figure 1C). Further, eosinophils were significantly increased in mice undergoing heterologous infection compared to mice infected with RV-A1B on day six alone. RV-A2 infection on day 13 did not significantly increase eosinophils. There was an increase in lymphocytes in mice undergoing heterologous infection compared to the other groups (Figure 1C).

To determine whether enhanced type 2 inflammatory responses in mice undergoing heterologous infection were due to increased viral load, we measured lung vRNA levels. First, RV-A1B and RV-A2 infections showed a similar time course of vRNA (Supplemental Figure 2A) and infectious virions were detected from mouse lungs infected with either strain (Supplemental Figure 2B). When we compared vRNA levels in mice infected with RV-A1B on day 6 and RV-A2 on day 13 with mice infected with RV-A2 on day 13 alone, mice undergoing heterologous infection unexpectedly showed a reduction in viral copies one day after RV-A2 infection (Figure 1D), suggesting early-life RV-A1B infection altered the immune response against subsequent RV-A2 infection. By days 2 and 7 after RV-A2 infection, there were no differences in viral RNA. Finally, there were no significant differences in *Il5*, *Il13*, *Muc5ac*, and *Muc5b* mRNA expression between male and female mice (Figure 1E).

We examined mice for PAS and Muc5ac staining, evidence of mucous metaplasia. As shown previously, RV-A1B infection on day 6 of life increased PAS staining compared to sham infection (Figure 2A). Since PAS detects glycoproteins, carbohydrates and mucins, staining indicates mucous metaplasia. Infection with RV-A2 on day 13 had no effect on PAS staining. The day 6-RV1B + day 13-RV-A2 treated mice showed significantly greater PAS staining compared to day 6-RV1B treated mice (Figure 2A). Similar results were obtained for deposition of the gel-forming mucin Muc5ac (Figures 2B, 2C), further evidence of mucus hypersecretion.

Heterologous infection with RV1B and RV-A2 induces ILC2 expansion and IL-13 production.

Next, we examined the effects of heterologous infection on lung ILC2 expansion. As shown previously [18], RV-A1B infection on day 6 of life increased lung lineage-negative CD25+, CD127+ ILC2s compared to sham infection. Heterologous infection with RV-A1B and RV-A2 increased lung ILC2 expansion compared to RV-A1B alone (Figure 3A and 3B). Furthermore, when we stained cells for IL-13, most of the IL-13-expressing cells were lineage-negative (Figures 3C). Heterologous infection with RV-A1B and RV-A2 increased the number of lung IL-13 expressing lineage-negative cells compared to RV-A1B alone (Figure 3D). However, heterologous infection also led to an increase in lung IL-13-expressing lineage-positive cells when compared to other groups (Figure 3D). When we measured IL-13 production from sorted lung ILC2s, PMA- and ionomycin-stimulated ILC2s

from lungs of RV-A1B + RV-A2-treated mice showed increased IL-13 production compared to cells from mice infected on with RV-A1B alone (Figure 3E). Similar results were obtained when cells were stimulated with IL-33, a physiologic agonist.

Finally, we assessed lung ILC2s by immunofluorescence microscopy. Mice infected with RV-A1B on day 6 of life demonstrated significantly increased lung IL-13-, GATA3- double positive, CD3-negative cells, consistent with lung ILC2 expansion (Figure 4A-C). Heterologous infection with RV-A2 on day 13 of life further augmented lung ILC2s. Heterologous infection also increased IL-13-, GATA3- and CD3-triple positive cells, suggesting IL-13 expression by Th2 cells.

As noted above, compared to sham-treated mice, mice infected with RV-A1B seven days before RV-A2 infection on day 13 of life failed to show a mature antiviral response, as evidenced by the absence of IFN-γ mRNA expression. These data suggest that early-life RV-A1B infection shifted the response to subsequent RV-A2 infection from a type 1 to type 2 response. To better characterize the effect of early-life RV-A1B infection on the immune response to subsequent heterologous RV infection, we compared airway responses of the sham + RV-A2 and RV-A1B + RV-A2 groups two days after RV-A2 infection. Compared to sham, preceding RV-A1B infection significantly reduced RV-A2-induced lung mRNA expression of CXCL1 and CXCL2 (Figure 5A). In contrast, prior RV-A1B infection increased mRNA expression of lung CCL11 and CCL24. Immunofluorescence imaging showed increased epithelial cell CCL11 protein expression (Figure 5B).

$Ror\alpha^{fl/fl}IL7R^{cre}$ lacking functional ILC2s demonstrate suppressed type 2 inflammation, eosinophilic inflammation, mucous metaplasia and airways responsiveness upon heterologous infection.

The *Rora*$^{fl/fl}$*Il7r*^{cre} mice lack functional ILC2s [25]. We infected the *Rora*$^{fl/fl}$*Il7r*^{cre} and *Rora*$^{fl/fl}$ mice with RV-A1B and determined ILC2 number by flow cytometry. *Rora*$^{fl/fl}$ mice showed expansion of lung ILC2s in response to RV-A1B treatment. *Rora*$^{fl/fl}$*IL7R*^{cre} showed almost a complete lack of ILC2s (Figure 6A). Next, we determined BAL inflammatory cell counts after RV-A1B and RV-A2 treatment. Eosinophils were significantly increased in RV-A1B-infected *Rora*$^{fl/fl}$ mice and further increased in *Rora*$^{fl/fl}$ mice infected RV-A1B on day 6 and RV-A2 on day 13 (Figure 6B). In contrast, *Rora*$^{fl/fl}$*Il7r*^{cre} mice showed almost a complete absence of eosinophils and mucus gene expression. *Rora*$^{fl/fl}$*Il7r*^{cre} mice also showed significant but incomplete suppression of IL-5, IL-13 and IL-4 compared to *Rora*$^{fl/fl}$ mice upon heterologous infection (Figure 6C). *Rora*$^{fl/fl}$*Il7r*^{cre} mice showed no decrement in TNF-α or IL-12 mRNA expression, demonstrating that ILC2s are not responsible for these cytokines. *Rora*$^{fl/fl}$*Il7r*^{cre} mice appeared to show a slight increase in viral copy number seven days after infection (Figure 6D). Finally, day 6 RV1B + day 13 RV-A2-infected *Rora*$^{fl/fl}$*Il7r*^{cre} mice showed an absence of PAS staining (Figure 6E) or airways responsiveness (Figure 6F) compared to similarly-treated *Rora*$^{fl/fl}$ mice.

Discussion

Early-life wheezing-associated respiratory tract infection by RV is considered a risk factor for asthma development [1-5]. Children are infected with many different RV strains, with

infants having 6-10 distinct RV infections per year [8]. RV infections do not induce specific immunity to reinfection by heterologous serotypes, even if viruses are from the same species, for example RV-A1A and RV-A2 [9, 10]. Recurrent RV infections could result in greater degrees of airway inflammation and the potential for airway remodeling and loss of lung function over time. To test this, we infected wild type BALB/c mice with RV-A1B on day 6 of life and RV-A2 on day 13 of life. RV infection of 6 day-old mice, but not mature mice, induces an asthma-like phenotype which is associated with ILC2 expansion and dependent on IL-13, IL-25 and IL-33 [18]. We found that mice undergoing heterologous infection with RV-A1B and RV-A2 showed additive increases in IL-13, IL-5, IL-4, Gob5, Muc5b and Muc5ac, additive expansion of eosinophils and exaggerated mucus metaplasia compared to RV-A1B alone. These data demonstrate that successive RV infections can result in greater degrees of inflammation and mucus production than a single infection.

These results are more significant when examined in the context of development. We previously found that, examining the age-dependency of RV responses, RV induces IL-13 and IL-25 expression in 6 day-old mice, whereas mice 8 days and older show significant IFN-γ expression. Thus, as expected, mice infected with sham on day 6 of life and RV-A2 at day 13 of life showed mature antiviral responses. However, infection with RV-A1B on day 6 life shifted the response to later RV-A2 infection from a type 1 to type 2 response, as evidenced by increased IL-5 and IL-13 mRNA expression and reduced IFN-γ. In addition, compared to sham-infected mice, mice infected with RV-A1B on day 6 and RV-A2 on day 13 of life showed increased lung CCL11 and CCL24 and reduced CXCL1 and CXCL2 mRNA responses, consistent with the notion that early-life RV infection alters the host response to heterologous infection, causing a shift towards type 2 inflammation. However, mRNA expression of TNF and IL-12b was also exaggerated in mice infected with both RV-A1B and RV-A2, suggesting that heterologous infection does not strictly fit a type 2 model.

Successive infections with RV-A1B and RV-A2 increased lung mRNA expression of the IL-5, IL-13 and IL-4. ILC2s produce IL-4, IL-5 and IL-13 and are dependent on RORα and GATA3 for their development [26-30]. Accordingly, mice undergoing heterologous infection also showed significant expansion of CD25+ CD127+ ILC2s. Immunofluorescence imaging also showed expansion of IL-13+, GATA3+, CD3- cells around the airways. To test the requirement of ILC2s for eosinophilic inflammation and mucous metaplasia, we infected *Rora*$^{fl/fl}$*Il7r*^{cre} mice lacking functional ILC2s [25] as well as *Rora*$^{fl/fl}$ littermates. *Rora*$^{fl/fl}$*Il7r*^{cre} mice showed complete suppression of BAL eosinophils, mucous metaplasia and airways hyperresponsiveness compared to *Rora*$^{fl/fl}$ mice. We conclude that early-life heterologous infection with RV-A1B and RV-A2 induces an exaggerated asthma-like phenotype which is dependent on ILC2s.

ILC2s establish their presence in tissues primarily during early postnatal development [18, 31], and increases in tissue ILC2s following infection are mediated through local expansion [31]. Further, pulse-chase experiments in naïve adult mice show persistence of IL-5-producing ILC2s for at least four weeks, with a substantially lower rate of decay than labeled CD4+ T cells [32]. We found that ILC2s from lungs of RV-A1B + RV-A2-treated mice showed increased IL-13 production compared to cells from mice infected on with RV-A1B alone. It is therefore conceivable that lung ILC2s arising after the initial RV-A1B infection form a

stable population of innate immune cells capable of responding to subsequent infections, albeit in a non-specific manner. This concept of "trained immunity," *i.e.*, heterologous immunity attributable to innate immune memory, has been reviewed elsewhere [20]. Future studies, employing a longer gap between infections and fate mapping approaches [31], could answer this question.

Other cells besides ILC2s may be involved in the altered response to heterologous RV infection. Successive infection with RV-A1B and RV-A2 increased the number of lineage-positive IL-13-secreting GATA3+ CD3+ cells. In ILC2-deficient mice, the adaptive Th2 response to protease antigen was impaired due to the loss of ILC2-derived IL-13 which promoted dendritic cell migration to the draining lymph node [33] and production of the Th2 cell-attracting chemokine CCL17 [34]. ILC2s also express the co-stimulatory molecule OX40L which is needed for tissue-restricted T cell co-stimulation [35]. It is therefore possible that ILC2s cooperate with adaptive T helper type 2 cells to drive pathologic airway inflammation in response to heterologous viral infection. M2-polarized macrophages could also produce IL-5 and IL-13 in response to heterologous viral infection. In ovalbumin-treated mice, macrophages may produce IL-17 or IL-13 in response to RV-A1B infection, depending on their activation state [36]. Macrophages may also produce IL-5 and IL-13 in response to IL-25 and IL-33 [37]. IL-4/IL-13 production by CD4+ T cell and ILC2s activate M2 macrophages required for lung immunity against hookworms [38]. In asthmatic sputum, there is a positive correlation between numbers of ILC2s and numbers of M2-polarized macrophages, and co-culture of ILC2s with alveolar macrophages induced expression of M2 macrophage-related genes [39]. Finally, we also demonstrate that, compared to sham-infected mice, prior RV-A1B infection increases RV-A2-induced epithelial cell expression of CCL11, consistent with the notion that early-life RV infection directly or indirectly alters the response of epithelial cells to subsequent infection.

We would like to mention two limitations to our study. First, replication of human RV is minimal in mice. Species differences restrict replication, requiring a high inoculum. However, infection with RV-A1B increases lung type 1 IFN production and negative-strand viral RNA expression [22], markers of viral replication. Although replication is limited, the resulting host-induced innate immune response and immunopathology can still be studied. Indeed, replication-deficient viral vectors are a useful tool for studying the innate immune response to acute viral infection without ongoing cytopathic effects [40]. Second, it is difficult to compare the maturity of immature mice and human infants. While it may be surprising that six and 13 day-old mice, who are still nursing, demonstrate qualitatively different immune responses to viral infection, we have noted previously that the response to respiratory viral infection shifts from an immature type 2 response (characterized by IL-13 and IL-25) to a mature type 1 response (IFN-γ) around eight days of age [18]. In a subsequent study [41], we showed that IFN-γ treatment inhibits RV-induced ILC2 function and expansion, suggesting deficient IFN-γ production in 6 day-old mice permits RV-induced type 2 immune responses. Thus, breast feeding is just one indicator of maturity, and may not reflect structural or functional maturity of the lungs, nor the development of pulmonary immune function. [42]

We conclude that early-life heterologous infection with RV-A1B and RV-A2 induces intensified asthma-like phenotype consisting of airway eosinophilic inflammation and mucous metaplasia. Furthermore, early RV infection shifted the immune response to subsequent infection with a heterologous RV strain towards a type 2 response. This model, which is the first preclinical model to combine two early-life respiratory viral infections, may provide insight into the development of childhood asthma.

Supplementary Material

Refer to Web version on PubMed Central for supplementary material.

Acknowledgments

Funding: This work was supported NIH grant R01 AI120526 (to M.B. Hershenson)

Abbreviations:

ANOVA	analysis of variance
BAL	bronchoalveolar lavage
DAPI	4′,6-diamidino-2-phenylindole
RV	human rhinovirus
SEM	standard error of the mean
ILC2	type 2 innate lymphoid cell
PAS	periodic acid-Schiff

References

1. Kotaniemi-Syrjanen A, Vainionpaa R, Reijonen TM, Waris M, Korhonen K, Korppi M. Rhinovirus-induced wheezing in infancy--the first sign of childhood asthma? J Allergy Clin Immunol 2003; 111:66–71. [PubMed: 12532098]
2. Lemanske RF Jr, Jackson DJ, Gangnon RE, Evans MD, Li Z, Shult PA, et al. Rhinovirus illnesses during infancy predict subsequent childhood wheezing. J Allergy Clin Immunol 2005; 116:571–7. [PubMed: 16159626]
3. Jackson DJ, Gangnon RE, Evans MD, Roberg KA, Anderson EL, Pappas TE, et al. Wheezing rhinovirus illnesses in early life predict asthma development in high-risk children. Am J Respir Crit Care Med 2008; 178.
4. Rubner FJ, Jackson DJ, Evans MD, Gangnon RE, Tisler CJ, Pappas TE, et al. Early life rhinovirus wheezing, allergic sensitization, and asthma risk at adolescence. J Allergy Clin Immunol 2017; 139:501–7. [PubMed: 27312820]
5. Moraes TJ, Sears MR. Lower respiratory infections in early life are linked to later asthma. Thorax 2018; 73:105–6. [PubMed: 29170249]
6. Stein RT, Sherrill D, Morgan WJ, Holberg CJ, Halonen M, Taussig LM, et al. Respiratory syncytial virus in early life and risk of wheeze and allergy by age 13 years. Lancet 1999; 354:541–5. [PubMed: 10470697]
7. Sigurs N, Gustafsson PM, Bjarnason R, Lundberg F, Schmidt S, Sigurbergsson F, et al. Severe respiratory syncytial virus bronchiolitis in infancy and asthma and allergy at age 13. Am J Respir Crit Care Med 2005; 171:137–41. [PubMed: 15516534]

8. Kusel MM, de Klerk NH, Holt PG, Kebadze T, Johnston SL, Sly PD. Role of respiratory viruses in acute upper and lower respiratory tract illness in the first year of life: a birth cohort study. Pediatr Infect Dis J 2006; 25:680–6. [PubMed: 16874165]
9. Rosenbaum MJ, De Berry P, Sullivan EJ, Pierce WE, Mueller RE, Peckenpaugh RO. Epidemiology of the common cold in military recruits with emphasis on infections by rhinovirus types 1A, 2, and two unclassified rhinoviruses. Am J Epidemiol 1971; 93:183–93. [PubMed: 4326603]
10. Minor TE, Dick EC, Peterson JA, Docherty DE. Failure of naturally acquired rhinovirus infections to produce temporal immunity to heterologous serotypes. Infect Immun 1974; 10:1192–3. [PubMed: 16558111]
11. Durrani SR, Montville DJ, Pratt AS, Sahu S, DeVries MK, Rajamanickam V, et al. Innate immune responses to rhinovirus are reduced by the high-affinity IgE receptor in allergic asthmatic children. J Allergy Clin Immunol 2012; 130:489–95. [PubMed: 22766097]
12. van Meel ER, den Dekker HT, Elbert NJ, Jansen PW, Moll HA, Reiss IK, et al. A population-based prospective cohort study examining the influence of early-life respiratory tract infections on school-age lung function and asthma. Thorax 2018; 73:167–73. [PubMed: 29101282]
13. Jackson DJ, Gangnon RE, Evans MD, Roberg KA, Anderson EL, Pappas TE, et al. Wheezing rhinovirus illnesses in early life predict asthma development in high-risk children. Am J Respir Crit Care Med 2008; 178:667–72. [PubMed: 18565953]
14. Oddy WH, de Klerk NH, Sly PD, Holt PG. The effects of respiratory infections, atopy, and breastfeeding on childhood asthma. Eur Respir J 2002; 19:899–905. [PubMed: 12030731]
15. Kusel MMH, de Klerk NH, Kebadze T, Vohma V, Holt PG, Johnston SL, et al. Early-life respiratory viral infections, atopic sensitization, and risk of subsequent development of persistent asthma. J Allergy Clin Immunol 2007; 119:1105–10. [PubMed: 17353039]
16. Culley FJ, Pollott J, Openshaw PJM. Age at first viral infection determines the pattern of T cell–mediated disease during reinfection in adulthood. J Exp Med 2002; 196:1381–6. [PubMed: 12438429]
17. Dakhama A, Park J-W, Taube C, Joetham A, Balhorn A, Miyahara N, et al. The enhancement or prevention of airway hyperresponsiveness during reinfection with respiratory syncytial virus is critically dependent on the age at first infection and IL-13 production. J Immunol 2005; 175:1876–83. [PubMed: 16034131]
18. Hong JY, Bentley JK, Chung Y, Lei J, Steenrod JM, Chen Q, et al. Neonatal rhinovirus induces mucous metaplasia and airways hyperresponsiveness through IL-25 and type 2 innate lymphoid cells. J Allergy Clin Immunol 2014; 134:429–39. [PubMed: 24910174]
19. Han M, Rajput C, Hong JY, Lei J, Hinde JL, Wu Q, et al. The innate cytokines IL-25, IL-33, and TSLP cooperate in the induction of type 2 innate lymphoid cell expansion and mucous metaplasia in rhinovirus-infected immature mice. J Immunol 2017; 199:1308–18. [PubMed: 28701507]
20. Dowling DJ, Levy O. Ontogeny of early life immunity. Trends Immunol 2014; 35:299–310. [PubMed: 24880460]
21. Tuthill TJ, Papadopoulos NG, Jourdan P, Challinor LJ, Sharp NA, Plumpton C, et al. Mouse respiratory epithelial cells support efficient replication of human rhinovirus. J Gen Virol 2003; 84:2829–36. [PubMed: 13679617]
22. Newcomb DC, Sajjan US, Nagarkar DR, Wang Q, Nanua S, Zhou Y, et al. Human rhinovirus 1B exposure induces phosphatidylinositol 3-kinase-dependent airway inflammation in mice. Am J Respir Crit Care Med 2008; 177:1111–21. [PubMed: 18276942]
23. Martin S, Casasnovas JM, Staunton DE, Springer TA. Efficient neutralization and disruption of rhinovirus by chimeric ICAM-1/immunoglobulin molecules. J Virol 1993; 67:3561–8. [PubMed: 8098781]
24. Tsai WC, Rodriguez ML, Young KS, Deng JC, Thannickal VJ, Tateda K, et al. Azithromycin blocks neutrophil recruitment in pseudomonas endobronchial infection. Am J Respir Crit Care Med 2004; 170:1331–9. [PubMed: 15361366]
25. Oliphant CJ, Hwang YY, Walker JA, Salimi M, Wong SH, Brewer JM, et al. MHCII-mediated dialog between group 2 innate lymphoid cells and CD4(+) T cells potentiates type 2 immunity and promotes parasitic helminth expulsion. Immunity 2014; 41:283–95. [PubMed: 25088770]

26. Halim TF, MacLaren A, Romanish MT, Gold MJ, McNagny KM, Takei F. Retinoic-acid-receptor-related orphan nuclear receptor alpha is required for natural helper cell development and allergic inflammation. Immunity 2012; 37:463–74. [PubMed: 22981535]
27. Klein Wolterink RG, Serafini N, van Nimwegen M, Vosshenrich CA, de Bruijn MJ, Fonseca Pereira D, et al. Essential, dose-dependent role for the transcription factor Gata3 in the development of IL-5+ and IL-13+ type 2 innate lymphoid cells. Proc Natl Acad Sci USA 2013; 110:10240–5. [PubMed: 23733962]
28. KleinJan A, Klein Wolterink RG, Levani Y, de Bruijn MJ, Hoogsteden HC, van Nimwegen M, et al. Enforced expression of Gata3 in T cells and group 2 innate lymphoid cells increases susceptibility to allergic airway inflammation in mice. J Immunol 2014; 192:1385–94. [PubMed: 24415780]
29. Noval Rivas M, Burton OT, Oettgen HC, Chatila T. IL-4 production by group 2 innate lymphoid cells promotes food allergy by blocking regulatory T-cell function. J Allergy Clin Immunol 2016; 138:801–11.e9. [PubMed: 27177780]
30. Pelly VS, Kannan Y, Coomes SM, Entwistle LJ, Rückerl D, Seddon B, et al. IL-4-producing ILC2s are required for the differentiation of TH2 cells following Heligmosomoides polygyrus infection. Mucosal Immunol 2016; 9:1407. [PubMed: 26883724]
31. Schneider C, Lee J, Koga S, Ricardo-Gonzalez RR, Nussbaum JC, Smith LK, et al. Tissue-resident group 2 innate lymphoid cells differentiate by layered ontogeny and in situ perinatal priming. Immunity 2019; 50:1425–38.e5. [PubMed: 31128962]
32. Nussbaum JC, Van Dyken SJ, von Moltke J, Cheng LE, Mohapatra A, Molofsky AB, et al. Type 2 innate lymphoid cells control eosinophil homeostasis. Nature 2013; 502:245–8. [PubMed: 24037376]
33. Halim TY, Steer CA, Mathä L, Gold MJ, Martinez-Gonzalez I, McNagny KM, et al. Group 2 innate lymphoid cells are critical for the initiation of adaptive T helper 2 cell-mediated allergic lung inflammation. Immunity 2014; 40:425–35. [PubMed: 24613091]
34. Halim TY, Hwang YY, Scanlon ST, Zaghouani H, Garbi N, Fallon PG, et al. Group 2 innate lymphoid cells license dendritic cells to potentiate memory TH2 cell responses. Nature Immunol 2015; 17:57. [PubMed: 26523868]
35. Halim TY, Rana BM, Walker JA, Kerscher B, Knolle MD, Jolin HE, et al. Tissue-restricted adaptive type 2 immunity is orchestrated by expression of the costimulatory molecule OX40L on group 2 innate lymphoid cells. Immunity 2018; 48:1195–207.e6. [PubMed: 29907525]
36. Hong JY, Chung Y, Steenrod J, Chen Q, Lei J, Comstock AT, et al. Macrophage activation state determines the response to rhinovirus infection in a mouse model of allergic asthma. Respir Res 2014; 15:63. [PubMed: 24907978]
37. Yang Z, Grinchuk V, Urban JF Jr., Bohl J, Sun R, Notari L, et al. Macrophages as IL-25/IL-33-responsive cells play an important role in the induction of type 2 immunity. PLoS One 2013; 8:e59441. [PubMed: 23536877]
38. Bouchery T, Kyle R, Camberis M, Shepherd A, Filbey K, Smith A, et al. ILC2s and T cells cooperate to ensure maintenance of M2 macrophages for lung immunity against hookworms. Nature Commun 2015; 6:6970. [PubMed: 25912172]
39. Kim J, Chang Y, Bae B, Sohn K-H, Cho S-H, Chung DH, et al. Innate immune crosstalk in asthmatic airways: Innate lymphoid cells coordinate polarization of lung macrophages. J Allergy Clin Immunol 2019; 143:1769–82.e11. [PubMed: 30414858]
40. Lee BH, Hwang DM, Palaniyar N, Grinstein S, Philpott DJ, Hu J. Activation of P2X7 receptor by ATP plays an important role in regulating inflammatory responses during acute viral infection. PLoS One 2012; 7:e35812. [PubMed: 22558229]
41. Han M, Hong JY, Jaipalli S, Rajput C, Lei J, Hinde JL, et al. IFN-γ blocks development of an asthma phenotype in rhinovirus-infected baby mice by inhibiting type 2 innate lymphoid cells. Am J Respir Cell Mol Biol 2017; 56:242–51. [PubMed: 27679954]
42. Lewin G, Hurtt ME. Pre- and postnatal lung development: An updated species comparison. Birth Defects Res 2017; 109:1519–39. [PubMed: 28876535]

Key Messages:

- Early-life (day 6) human rhinovirus (RV) infection of immature mice induces eosinophilic inflammation and mucous metaplasia whereas later infection (day 13) induces a mature type 1 antiviral response.
- Early-life infection with RV-A1B skews the immune response to subsequent heterologous infection with RV-A2, causing an exaggerated asthma phenotype unrelated to increased viral load.
- Type 2 innate lymphoid cells are required for exaggerated eosinophilic inflammation and mucous metaplasia due to heterologous RV infections.

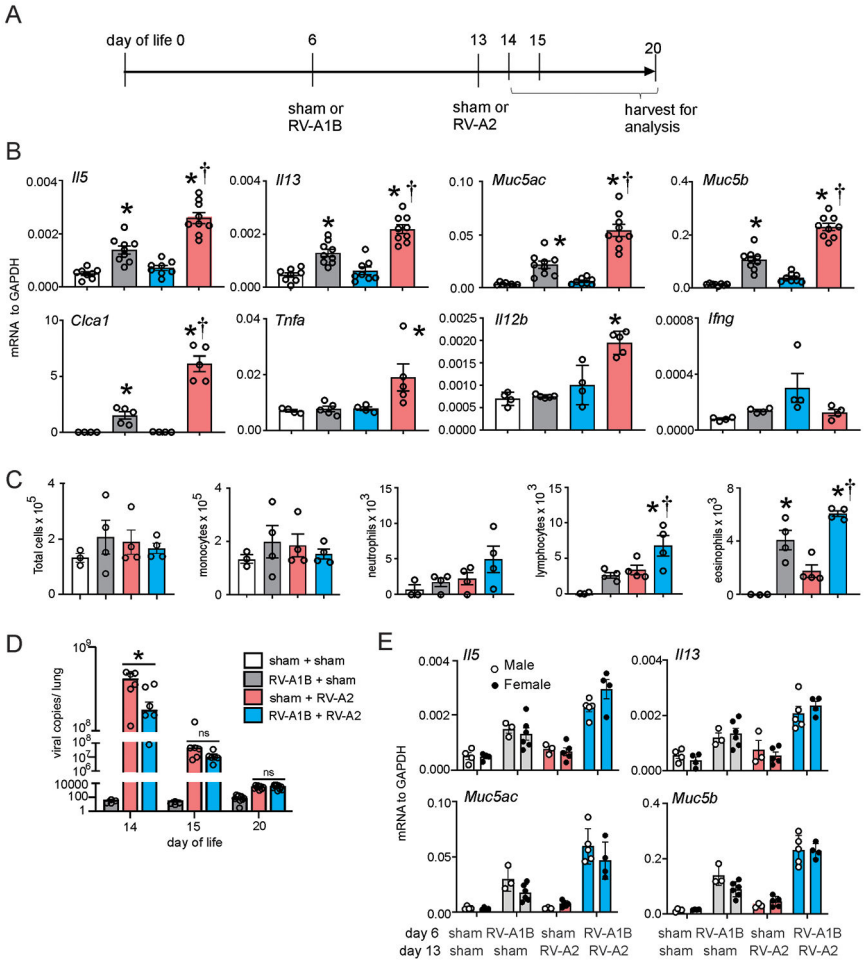

Figure 1. Heterologous RV infection induces exaggerated airway responses.

A) Baby mice were inoculated with sham or RV-A1B or on day 6 of life and sham or RV-A2 on day 13 of life. B) Lungs from sham + sham, sham + RV-A1B, sham + RV-A2, and RV-A1B + RV-A2-infected mice were harvested on day 20 of life. Shown is lung mRNA expression of IL-5, IL-13, IL-5, IFN-γ, Gob5 (*Clca1*), Muc5b, Muc5ac, TNF-α and IL-12b. C) BAL inflammatory cell counts for sham + sham, sham + RV-A1B, sham + RV-A2, and RV-A1B + RV-A2-infected mice. Data shown are mean ± SEM; n=3-9/group from two different experiments; *different from sham + sham, †different from RV-A1B + sham, $P < 0.05$ by one-way ANOVA and Tukey multiple comparison test. D) RV positive-strand RNA was measured on days 14, 15 or 20 of age (1, 2 or 7 days post RV-A2 infection), and presented as viral copy number in total lung. Data shown are mean±SEM, N =4-9, *different from day-6-sham + day-13-RV-A2, p<0.05, one-way ANOVA and Tukey multiple comparison test. E) mRNA expression in male and female mice.

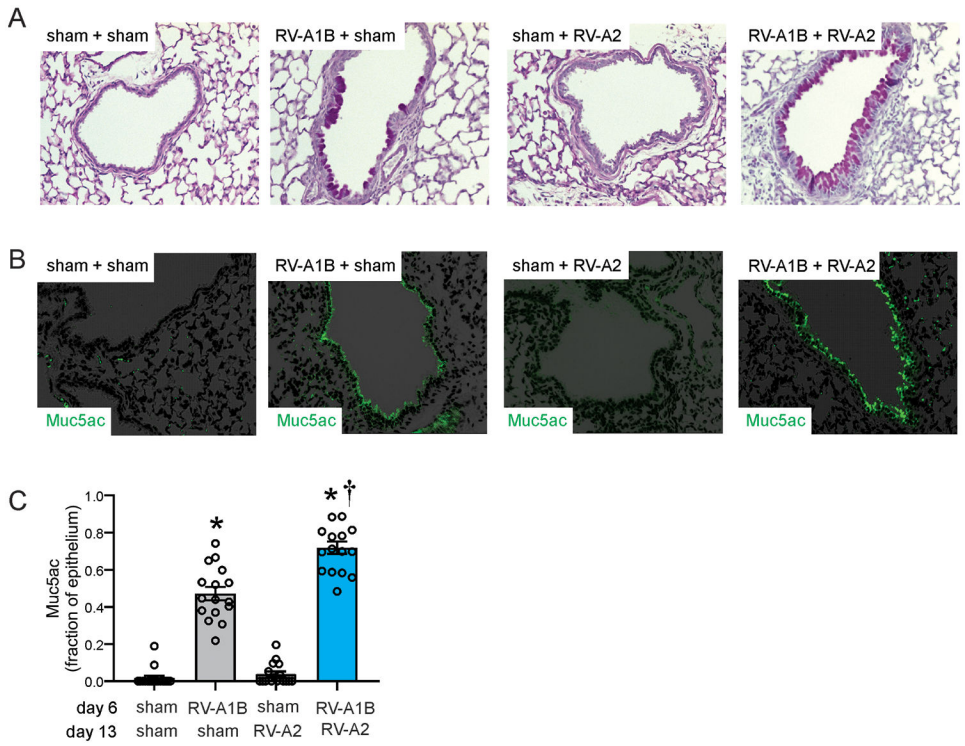

Figure 2. Heterologous RV infection induces exaggerated mucus metaplasia.

Baby mice were inoculated with sham or RV-A1B on day 6 and sham or RV-A2 on day 13 of life. Lungs were harvested on day 20 and processed for histology. Lungs sections were stained for PAS and Muc5ac and quantified using NIH ImageJ. A) PAS staining in sham, RV-A1B, RV-A2, RV-A1B + RV-A2-infected mice. The black bar is 50 microns (μ). B) Muc5ac staining in RV-A1B, RV-A2, RV1B + RV-A2-infected mice. The white bar is 50 μ. C) Quantification of Muc5ac staining in the airways. Data are represented are Muc5ac-positive cells per micron of basement membrane length. Images were taken at ×200 magnification. Data shown are mean ± SEM; n=3-4 airways/mouse, 4 mice per group from two different experiments; *different from sham + sham, †different from RV-A1B + sham, $P < 0.05$ by one-way ANOVA and Tukey multiple comparison test.

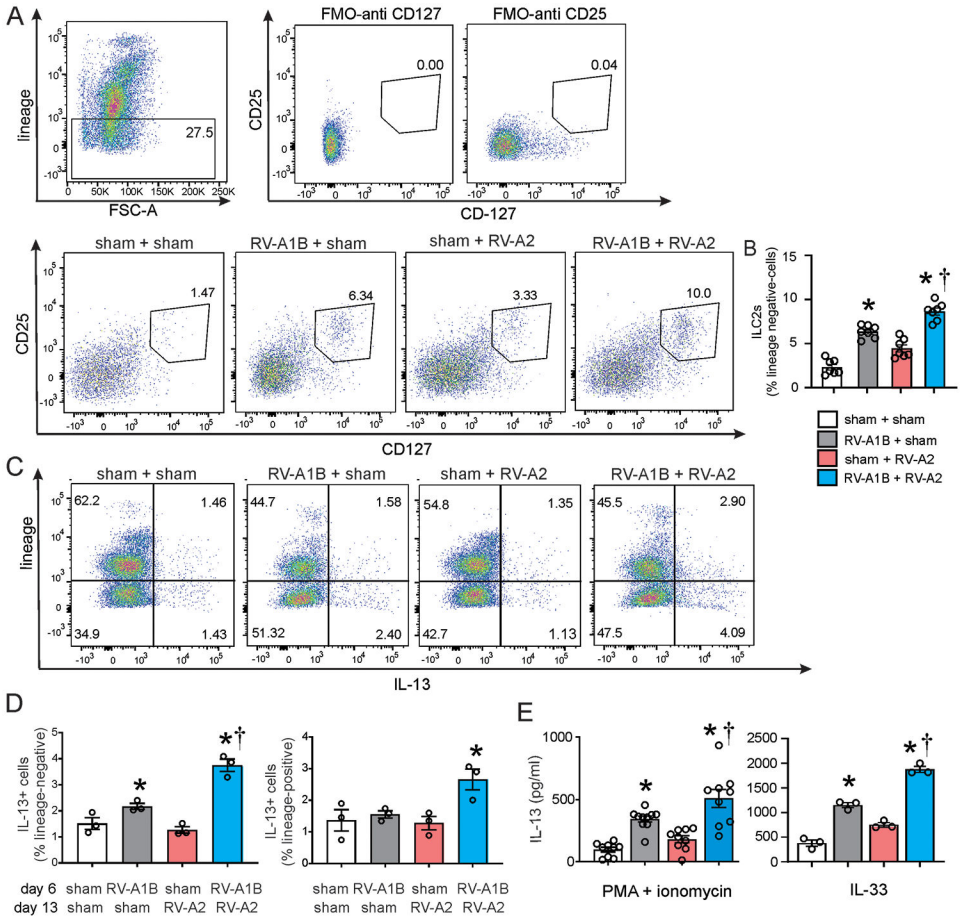

Figure 3. RV infection induces ILC2 expansion.

A) Figure showing flow cytometry analysis of live lineage-negative, CD25+ CD127+ ILC2s. B) Graph showing group mean data for ILC2s. Data shown are mean ± SEM; n=7 per group from three different experiments; *different from sham + sham, †different from RV-A1B + sham, $P < 0.05$ by one-way ANOVA and Tukey multiple comparison test. C) Flow cytometry analysis of lineage markers and IL-13 in sham, RV-A1B, RV-A2 and RV-A1B + RV-A2 groups. D) Lineage-negative, IL-13+ cells (left panel) and lineage-positive, IL-13+ cells (right panel) for the four groups. Data are mean ± SEM; n=3 per group from one experiment; *different from sham + sham, †different from RV-A1B + sham, P < 0.05 by one-way ANOVA and Tukey multiple comparison test. E) IL-13 production from sorted lineage-negative, CD25+, CD127+ ILC2s. ILC2s were stimulated with either PMA and ionomycin (left panel) or IL-33 (right panel). Data shown are mean ± SEM; n = 9-10 per group from three experiments for PMA and ionomycin stimulation; n=3 per group from one experiment for IL-33 stimulation; *different from sham + sham, †different from RV-A1B + sham, P < 0.05 by one-way ANOVA and Tukey multiple comparison test

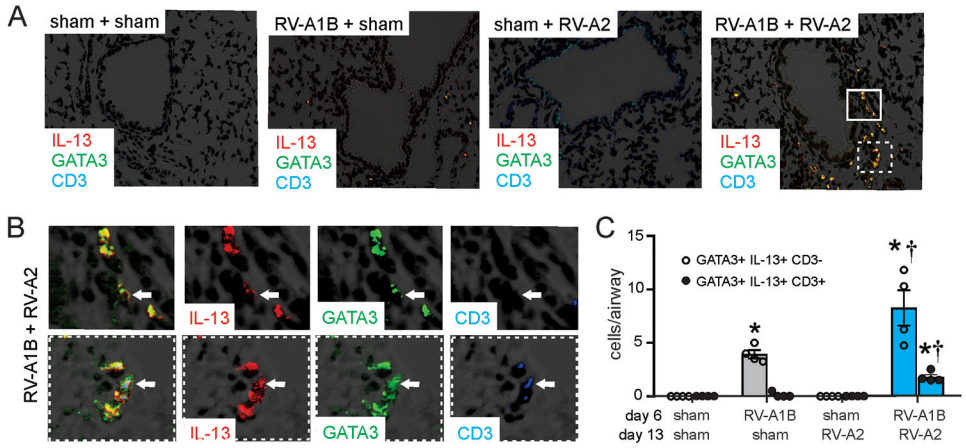

Figure 4. Airway immunofluorescence staining for IL-13, GATA3 and CD3.

Baby mice were inoculated with sham or RV-A1B on day 6 of life and sham or RV-A2 on day 13 of life. On day 20, lungs were harvested and fixed with paraformaldehyde. A) Lung sections were stained with anti-IL-13 (shown in red) anti-GATA3 (green), anti-CD3 (blue) and DAPI (black). Areas of IL-13 and GATA3 colocalization appear yellow; areas of GATA3 and CD3 colocalization appear cyan (if IL-13-negative) or white (if IL-13-positive). The white bar is 50 μ. B) Color breakdown of areas outlined in panel A. Solid box outlines IL-13+ GATA3+ CD3-negative cells; dashed box outlines IL-13+ GATA3+ CD3+ cells. The white bar is 10 μ. C) Group mean data showing IL-13+ GATA3+ CD3-negative (open bars) and CD3+ (shaded bars). Each point represents the average of four airways from one mouse. Data shown are mean ± SEM; *different from sham + sham, †different from RV-A1B + sham, $P < 0.05$ by one-way ANOVA and Tukey multiple comparison test.

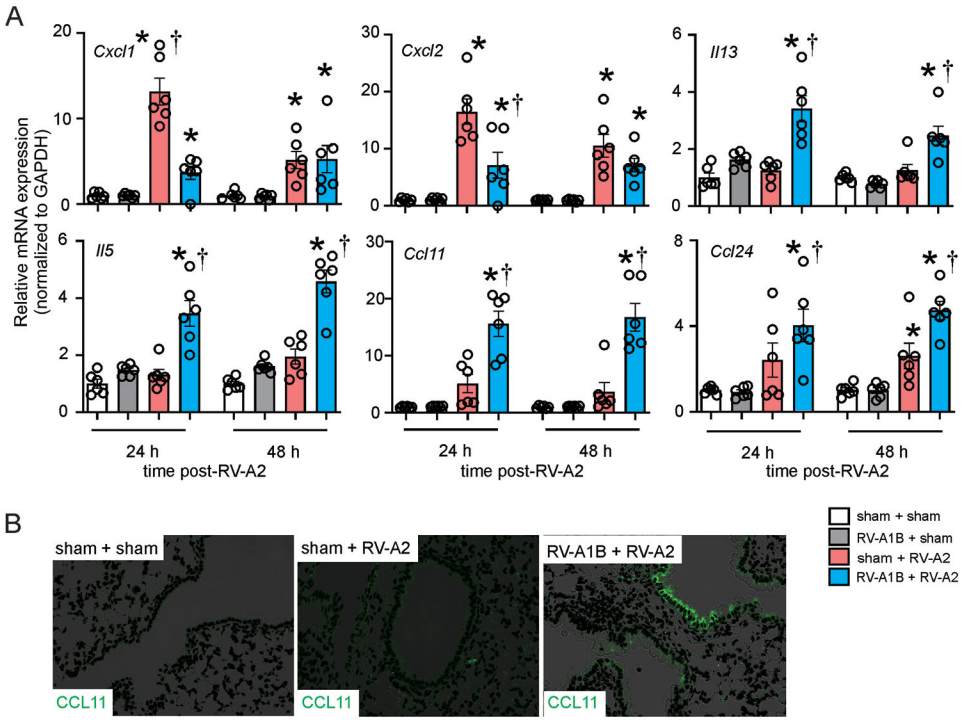

Figure 5. Effect of prior RV-A1B infection on the response to heterologous infection with RV-A2.

Baby mice were inoculated with sham or RV-A1B on day 6 of life and sham or RV-A2 on day 13 of life. On days 14 and 15, *i.e.,* 24 and 48 h after RV-A2 infection, lungs were harvested for mRNA analysis by qPCR or lung immunofluorescence staining. A) mRNA expression of CXCL1, CXCL2, IL-13, IL-5, CCL11 and CCL24. Gene expression values were normalized to GAPDH and represented as fold increase over sham + sham inoculated mice. Data are mean ± SEM; n=6 per group from two different experiments; *different from sham + RV-A2, $P < 0.05$ by one-way ANOVA and Tukey multiple comparison test. B) Lung sections were stained with anti-CCL11 (shown in green; the white bar is 50 μ).

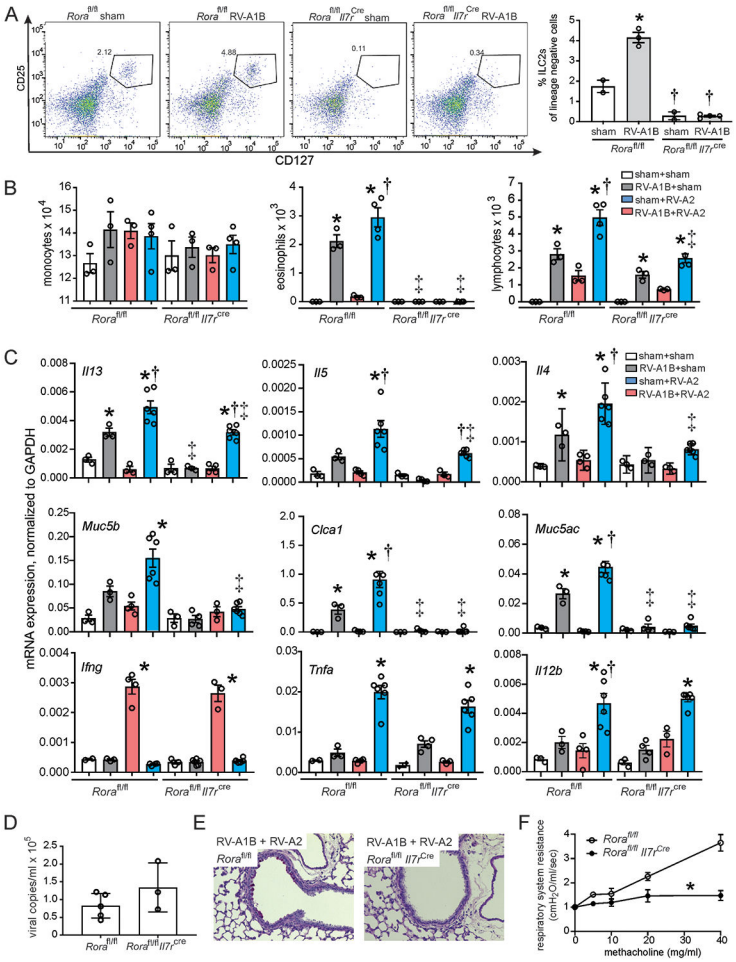

Figure 6. Rora$^{fl/fl}$Il7r^{cre} ILC2-deficient mice are protected from heterologous infection induced exaggerated type 2 inflammation and mucous metaplasia.

A) Flow cytometry analysis of lineage-, CD25+, CD127+ ILC2s. N=2-4 per group B) BAL inflammatory cell counts and C) mRNA expression in sham + sham, RV-A1B + sham, sham + RV-A2 and RV-A1B + RV-A2-infected *Rora*$^{fl/fl}$ and *Rora*$^{fl/fl}$*Il7r*^{cre} ILC2-deficient mice. For panels B and C, N=3-6 per group. For panels A-C, data are mean ± SEM; *different from sham + sham group of like mouse strain, †different from RV-A1B + sham of like mouse strain, ‡different from corresponding group in *Rora*$^{fl/fl}$ mouse strain, P < 0.05 by one-way ANOVA and Tukey multiple comparison test. D). Viral copy number in RV-A1B + RV-A2-infected *Rora*$^{fl/fl}$ and *Rora*$^{fl/fl}$*Il7r*^{cre} ILC2-deficient mice. E. PAS-stained representative airways from RV-A1B + RV-A2-infected *Rora*$^{fl/fl}$ mice (left) and *Rora*$^{fl/fl}$*Il7r*^{cre} ILC2-deficient mice (right). The black bar is 50 μ. F) Changes in total respiratory system resistance in response to inhaled methacholine in anesthetized, tracheotomized *Rora*$^{fl/fl}$ and *Rora*$^{fl/fl}$*Il7r*^{cre} mice. Resistance data were normalized to baseline airways resistance. Data are mean ± SEM for 3-10 per group measured in 3 different experiments, *different from *Rora*$^{fl/fl}$ mice, $P < 0.05$ by two-way ANOVA and Tukey multiple comparison test.